

Trickle-Bed Reactors: Liquid Diffusional Effects in a Gas-Limited Reaction

A model is developed for predicting the performance of a partially wetted trickle-bed reactor for a gas-limiting reaction of order less than or equal to one. The model indicates that under certain conditions the liquid reactant may affect the reaction rate due to its inability to rapidly diffuse to catalyst areas that are in direct contact with the gas. This model is the first to explain and predict on a rational basis the experimental results for the hydrogenation of diluted α -methylstyrene and aqueous maleic acid reported in the literature. A criterion that determines when liquid reactant effects can be expected is developed and reported.

E. G. Beaudry, M. P. Duduković
Chemical Reaction Engineering Laboratory
Washington University
St. Louis, MO 63130

P. L. Mills
Corporate Research Laboratories
Monsanto Company
St. Louis, MO 63167

Introduction

Reactions occurring in trickle-bed reactors, where gas and liquid reactants flow cocurrently downward over a packed bed of catalyst, can often be classified into liquid-reactant limited and gas-reactant limited (Mills and Duduković, 1980). The former are frequently encountered in high-pressure operations in petroleum processing. The latter occur when there is a non-volatile liquid reactant and a slightly soluble gas, as in some oxidations and partial hydrogenations of chemicals at low and moderate pressures. Here we concern ourselves only with such gas-limited reactions.

It has been well established that at low liquid mass velocities, below 3 to 5 kg/m² · s, the trickling liquid does not actively wet the entire external catalyst surface in the bed. The pertinent literature was summarized by Duduković and Mills (1986). For such conditions of partial external catalyst wetting, several models have been proposed for evaluation of the catalyst effectiveness factor (Duduković and Mills, 1978; Herskowitz et al., 1979; Ramachandran and Smith, 1979; Mills and Duduković, 1980; Levec et al., 1980; Tan and Smith, 1980; Martinez et al., 1981; Herskowitz, 1981; Goto et al., 1981; Capra et al., 1982; Sakornwimon and Sylvester, 1982; Ring and Missen, 1984). All of these models predict that the observed reaction rate increases as catalyst contacting efficiency decreases for a nonvolatile liquid in a gas-limited reaction. Here the contacting efficiency is defined to be the fraction of external catalyst area actively wetted by liquid. The above is intuitively acceptable based on the following argument. Since the liquid reactant is nonvolatile, reaction can occur only in the wetted interior of catalyst pellets. The gas reactant must overcome both the gas-liquid and liquid-solid mass transfer resistances of the flowing liquid film to penetrate into a completely wetted catalyst pellet. A pellet with a partially dry surface provides a much smaller resistance at the dry surface for the gas to access the liquid-filled pore volume

and react. At higher Thiele moduli, when the reaction rate is large compared to the internal diffusion rate, external mass transfer effects greatly affect the observed reaction rate. The reduction of the mass transfer resistance for the rate-limiting gaseous reactant on partially wetted pellets leads to higher observed reaction rates. These model predictions have been found to be in good agreement with a number of experimental observations on differential trickle beds for the hydrogenation of α -methylstyrene in cumene (Morita and Smith, 1978; Herskowitz et al., 1979) and the oxidation of sulfur dioxide (Mata and Smith, 1981).

The above models fail to predict or explain some other experimental observations. For example, those models greatly overpredict the reaction rate on partially wetted palladium-on-alumina catalyst for the hydrogenation of dilute α -methylstyrene in various organic solvents (El-Hisnawi, 1981; El-Hisnawi et al., 1982; Mills et al., 1984). El-Hisnawi (1981) had determined a zero-order dependence of this reaction on α -methylstyrene concentration and first-order dependence with respect to hydrogen in a slurry and stirred-basket reactor where the catalyst is completely wetted. Yet, a positive-order dependence on the α -methylstyrene concentration seemed apparent in his trickle-bed experiments. In order to fit a model to such data, Mills and Duduković (1984) had to assume that the dry or inactively wetted portion of the catalyst surface offered a significant resistance to the transport of the gas reactant. This is in complete contrast to the assumption of negligible resistance used by other investigators (Morita and Smith, 1978; Herskowitz et al., 1979; Tan and Smith, 1980; Sakornwimon and Sylvester, 1982; Capra et al., 1982). While a good fit was obtained by Mills and Duduković (1984) for a catalyst of one activity, no general predicta-

Correspondence concerning this paper should be addressed to E. G. Beaudry.

bility of the model for catalysts of different activities was achieved.

Ruiz et al. (1984), studying the hydrogenation of aqueous nonvolatile maleic acid, found a variable rate dependence on the maleic acid concentration. The rate was almost zero order (0.06 order) with respect to the liquid reactant and 0.6 order with respect to hydrogen in a stirred-basket reactor. This reaction rate, determined in a differential partially wetted trickle-bed reactor, showed strong dependencies on the maleic acid concentration (about 0.3 order) that the authors could not explain. Unconvincing arguments were made that small variations in the feed concentrations of maleic acid can cause great variations in wetting efficiency, which in turn resulted in different apparent reaction rates.

The objective of this paper is to present a rational model, based on first principles, that can explain all the experimental observations encountered so far with gas-limited reactions, of order one or less, in partially wetted trickle beds. We start with the realization that the previous models considered only the supply of the limiting gas reactant to the partially wetted pellet by usually assuming a negligible mass transfer resistance on the dry surface and a substantial resistance on the actively wetted surface. Since the product of the effective diffusivity and bulk concentration for the zero-order liquid reactant was many times greater than the product of those two quantities for the gas reactant, which guarantees that the liquid reactant will not be depleted in a totally wetted pellet, any possible effect of the liquid reactant was *a priori* dismissed. We will show here that under such conditions a partially wetted pellet can become starved for the liquid reactant and that the presumed zero-order reactant may start affecting the rate.

The nonvolatile liquid reactant is only supplied to the pellet from the actively wetted surface. Its diffusion toward the dry (or inactively wetted) catalyst surfaces, where the gas reactant is abundant due to the negligible external resistance, may limit the reaction rate, especially when the intraparticle diffusion resistance is significant (large Thiele modulus) and the nonvolatile reactant is dilute. Under such conditions, sections of the catalyst near the dry surface become starved for the nonvolatile liquid reactant, rendering a fraction of the catalyst useless. The gas reactant must penetrate through this layer depleted of the liquid reactant, and this creates the unexpectedly high apparent mass transfer resistance on dry surfaces, as accounted for by Mills and Duduković (1984). This possible physical explanation was independently suggested by Harriott (1984). It can explain the increased dependence of the reaction rate on the nonvolatile reactant observed in the partially wetted trickle beds referenced above.

We proceed to show that a model based on the described physical concepts quantitatively predicts experimental observations. We formulate first a model for a partially wetted pellet, followed by a statistical model for the partially irrigated bed, and then compare the trickle-bed model predictions with literature data.

Particle Model

Assumptions

The simplest geometry for a partially wetted pellet is an infinite slab with one side actively wetted and the other side dry (or inactively wetted) as shown in Figure 1 for an external shell cat-

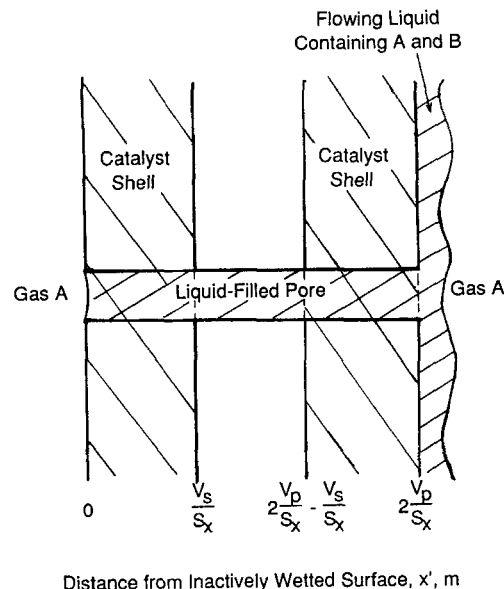


Figure 1. Half-wetted external shell catalyst modeled as an infinite slab.

alyst. This geometry was first used to model a partially wetted trickle-bed reactor by Tan and Smith (1980), but only the mass balance of one volatile reactant was considered. Since the effects to be described here are important at large Thiele moduli, the slab geometry is an adequate representation of other more complex particle shapes if a normalized modulus is used. This pellet geometry reduces each reactant mass balance to an equation of one-dimensional diffusion with reaction. The following assumptions, all applicable to the α -methylstyrene and maleic acid hydrogenations, were made for the particle-scale model to determine if the nonvolatile zero-order reactant *B* can start affecting the heterogeneous catalytic reaction with otherwise gas-limiting reactant *A*. The development is presented for a shell-type catalyst. A uniform catalyst is just a subcase of the solution presented.

1. The slab is of characteristic width $2V_p/S_x$ and the characteristic depth of the external catalyst shell is V_s/S_x , where V_p and V_s are the volumes of the pellet and external catalyst shell, respectively, and S_x is the pellet external surface area. For a catalyst with the metal uniformly distributed throughout, the pellet and shell volumes are identical: $V_p = V_s$.

2. The reaction is irreversible, independent of all product concentrations, and of order m with respect to the dissolved gas reactant (*A*) concentration, where m is less than or equal to one and greater than zero. This reactant can be supplied to the pellet from either side.

3. The reaction is strictly zero order with respect to the nonvolatile reactant *B*. This nonvolatile reactant can only be supplied to the pellet from the actively wetted side.

4. The pellet is isothermal and at steady state.

5. There are no bulk motion contributions to the mass balances and the effective diffusivities of the reactants are constant.

6. The pellet is completely internally wetted.

7. The flowing liquid concentration of *B* times its effective diffusivity is much greater than that of dissolved *A* times its

effective diffusivity. If this were not true, then B could limit the reaction rate even in a completely wetted pellet. This assumption insures that if B is depleted within the catalyst pellet, it is depleted on the pellet half nearer the inactively wetted surface.

8. The intrinsic kinetic rate is much faster than the rate of intraparticle diffusion of the dissolved gas reactant. This means that the generalized Thiele modulus for the gas reactant, ϕ_A , is large, that is, greater than 4 for a first-order reaction and greater than $(1 + m)/(1 - m)$ for a reaction of order less than one. The case of large modulus is of primary interest and this assumption allows simpler analytical solutions to the equations.

Governing equations

Using the above assumptions, the following dimensionless differential equations model the profiles of the two reactants within the pellet:

$$\frac{d^2 C_A}{dx^2} - \frac{2}{m+1} (1 - \omega_x - \omega)^2 \phi_A^2 C_A^m = 0 \quad \text{for } 0 < x < 1 \quad (1)$$

$$\frac{d^2 C_B}{dx^2} - \frac{2}{m+1} (1 - \omega_x - \omega)^2 \delta \phi_A^2 \gamma C_A^m = 0 \quad \text{for } 0 < x < 1 \quad (2)$$

$$\frac{d^2 C_A}{dy^2} - \frac{2}{m+1} (1 - \omega_y)^2 \phi_A^2 C_A^m = 0 \quad \text{for } 0 < y < 1 \quad (3)$$

$$\frac{d^2 C_B}{dy^2} - \frac{2}{m+1} (1 - \omega_y)^2 \delta \phi_A^2 \gamma C_A^m = 0 \quad \text{for } 0 < y < 1 \quad (4)$$

where:

$$\omega_x = \omega_y = 0 \text{ if } m = 1$$

$$x = 1 - \frac{x' - \omega V_s/S_x}{(1 - \omega_x - \omega) V_s/S_x}$$

$$y = \frac{x' - 2V_p/S_x + (1 - \omega_y) V_s/S_x}{(1 - \omega_y) V_s/S_x}$$

$$\phi_A^2 = \left(\frac{V_s}{S_x} \right)^2 \frac{(m+1) k_{vs} (C_A^*)^{m-1}}{2 D_{eA}}$$

$$\delta = D_{eA}/D_{eB} \quad \gamma = b C_A^*/C'_{BL}$$

$$C_A = C'_A/C_A^* \quad C_B = C'_B/C'_{BL}$$

The term $\omega V_s/S_x$ is the distance measured from the dry (inactively wetted) surface to the plane at which the concentration of the liquid reactant B is depleted, as shown in Figures 2 and 3. If B is able to diffuse rapidly enough throughout the entire pellet, the value of ω is zero and the mass balance for a zero-order reactant B is unnecessary.

If the reaction is less than first order with respect to the concentration of the dissolved gas reactant A , the concentration of A will fall to zero within the catalyst shell for the assumed large ϕ_A . The term $(1 - \omega_x) V_s/S_x$ is then the distance from the dry (inactively wetted) surface to the plane at which the gas reac-

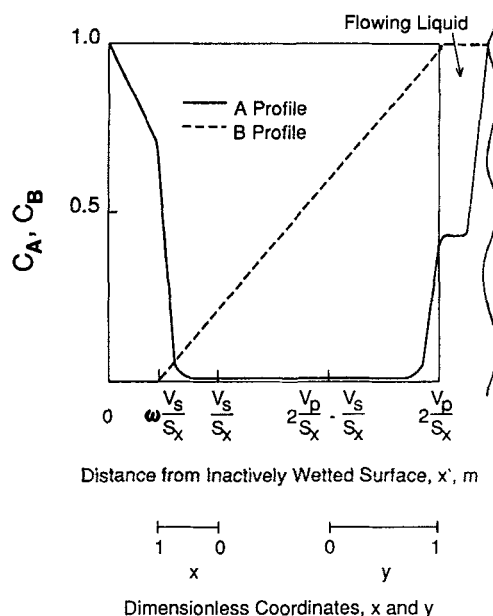


Figure 2. Possible concentration profiles at reactant B limiting conditions, $m = 1$.

tant entering from the dry surface is completely depleted. The term $(1 - \omega_y) V_s/S_x$ is the analogous distance from the actively wetted surface at which the gas reactant entering from that surface is depleted, as shown in Figure 3. For a first-order reaction ($m = 1$) both ω_x and ω_y are equal to zero, since the gas reactant A cannot be completely depleted.

The other terms in the above equations are straightforward and are defined in the Notation. The dimensional coordinate in

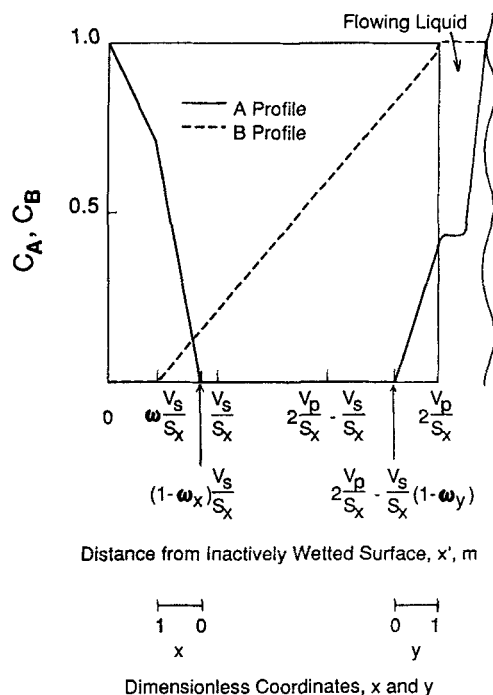


Figure 3. Possible concentration profiles at reactant B limiting conditions, $m < 1$.

the pellet measured from the inactively wetted surface is x' . The dimensionless coordinates, x and y , represent the reaction zones measured toward the inactively and actively wetted surfaces, respectively. D_e are the effective diffusivities, and C' and C are the dimensional and dimensionless liquid concentrations within the pellet, respectively. C_A^* is the dissolved dimensional concentration of reactant A in equilibrium with the gas, and k_{ws} is the intrinsic rate constant for a reaction of order m based on catalyst shell volume. C'_{BL} is the dimensional concentration of B in the flowing liquid, and b is the stoichiometric coefficient for the reactant B in the reaction $A + bB = \text{products}$.

Boundary conditions

Figure 2 shows possible reactant profiles in the pellet when B is completely depleted within the pellet and the reaction is first order in the gas concentration. The analogous situation, when the reaction is less than first order in the dissolved gas concentration, is shown in Figure 3. Recalling that ω_x and ω_y are zero for a first-order reaction in A , the following dimensionless boundary conditions are used:

$$\left. \frac{dC_A}{dx} \right|_{x=0} = - \frac{1 - \omega_x - \omega}{1 - \omega_y} \left. \frac{dC_A}{dy} \right|_{y=0} \quad (=0 \text{ for } m < 1) \quad (\text{BC1})$$

$$\left. \frac{dC_B}{dx} \right|_{x=0} = - \frac{1 - \omega_x - \omega}{1 - \omega_y} \left. \frac{dC_B}{dy} \right|_{y=0} \quad (\text{BC2})$$

$$C_A|_{x=0} = C_A|_{y=0} - 2 \left(\frac{V_p}{V_s} - 1 \right) \left. \frac{dC_A}{dy} \right|_{y=0} \quad (=0 \text{ for } m < 1) \quad (\text{BC3})$$

$$C_B|_{x=0} = C_B|_{y=0} - \frac{2(V_p/V_s - 1) + \omega_x + \omega_y}{1 - \omega_y} \left. \frac{dC_B}{dy} \right|_{y=0} \quad (\text{BC4})$$

$$\left. \frac{dC_A}{dy} \right|_{y=1} = (1 - \omega_y) Bi_{Ls,A} (C_{AL} - C_A|_{y=1}) \quad (\text{BC5})$$

$$\left. \frac{dC_B}{dy} \right|_{y=1} = (1 - \omega_y) Bi_{Ls,B} (1 - C_B|_{y=1}) \quad (\text{BC6})$$

$$\left. \frac{dC_A}{dx} \right|_{x=1} = \frac{1 - \omega_x - \omega}{\omega + 1/Bi_{gs,A}} (1 - C_A|_{x=1}) \quad (\text{BC7})$$

$$\left. \frac{dC_B}{dx} \right|_{x=1} = 0 \quad (\text{BC8})$$

$$C_B|_{x=1} = 0 \quad (\text{BC9})$$

where:

$$Bi = \frac{kV_s}{D_e S_x} \quad C_{AL} = C'_{AL}/C_A^*$$

Here BC1 and BC2 describe the continuity of fluxes of two reactants at the interior edges of the active catalyst shell; BC3 and BC4 represent the solution for the reactant concentration

profiles within the noncatalytic interior of the pellet; BC5, which is discussed in more detail in the paragraph below containing Eq. 5, and BC6 are the appropriate boundary conditions at the actively wetted surface; BC7–9 represent either the plane at which the concentration of B is depleted or the dry surface.

When the reaction is less than first order in the gas reactant A ($m < 1$), boundary conditions BC1 and BC3 are set equal to zero and provide the conditions necessary for determining the values of ω_x and ω_y . The last boundary condition, BC9, is always used to determine the value of ω . The terms C'_{AL} and C_{AL} are the dimensional and dimensionless concentrations of dissolved A in the flowing liquid, respectively. Bi and k are the modified Biot number for mass transfer and the mass transfer coefficient based on liquid concentration for the reactant, respectively. The subscript gs indicates gas-to-solid transfer at the dry (inactively wetted) surface, and the subscript Ls indicates flowing liquid-to-solid transfer at the actively wetted surface.

If the concentration of dissolved gas reactant A in the flowing liquid is constant, the flowing liquid concentration C_{AL} can be replaced by unity and the liquid-to-solid Biot number $Bi_{Ls,A}$ can be replaced by an overall gas-through-flowing-liquid-to-solid Biot number $Bi_{gLs,A}$ in boundary condition BC5. This overall Biot number is defined as follows:

$$Bi_{gLs,A} = \frac{V_s}{D_{eA} S_x} \left[\frac{1}{k_{Ls,A}} + \frac{\eta_{ce}(1 - \epsilon) S_x/V_p}{(Ka)_{gL,A}} \right]^{-1} \quad (5)$$

where ϵ is the bed porosity, $(Ka)_{gL,A}$ is the volumetric gas-to-liquid mass-transfer coefficient based on the dissolved gas concentration, and the external contacting (or wetting) efficiency is η_{ce} . These substitutions of unity for C_{AL} and of $Bi_{gLs,A}$ for $Bi_{Ls,A}$ are valid throughout the remainder of this paper.

Half-wetted Particle Overall Effectiveness Factor

The overall effectiveness factor for this dry-wet catalyst, defined as the observed rate divided by the rate that would be obtained if the equilibrium concentration of the dissolved gas reactant C_A^* were present throughout the catalyst shell, is given by:

$$\eta_{odw} = \frac{1}{2} \left[(1 - \omega_x - \omega) \int_0^1 C_A^m dx + (1 - \omega_y) \int_0^1 C_A^m dy \right] \quad (6)$$

Recall that ω_x and ω_y are both zero for a first-order reaction ($m = 1$).

Large ϕ_A solution for $m = 1$

For a first-order reaction when the generalized Thiele modulus is large ($\phi_A > 4$), $\tanh[\phi_A(1 - \omega)]$ and $\tanh(\phi_A)$ are approximately 1.0 and an explicit expression for Eq. 6 can be obtained. The intermediate results, before $\tanh[\phi_A(1 - \omega)]$ and $\tanh(\phi_A)$ have been replaced by 1.0, are given in the Appendix. The overall effectiveness factor is:

$$\eta_{odw} = \frac{1}{2\phi_A^2} \left(\frac{C_{AL}}{\phi_A + \frac{1}{Bi_{Ls,A}}} + \frac{1}{\omega + \frac{1}{\phi_A} + \frac{1}{Bi_{gs,A}}} \right) \quad (7)$$

The value of ω can be determined explicitly from the following equation:

$$\omega = \frac{2 \frac{V_p}{V_s} + \frac{1}{Bi_{Ls,B}} + \frac{1}{Bi_{gs,A}}}{\frac{1}{\phi_A} + \frac{1}{Bi_{gs,A}}} - \frac{1}{\phi_A} - \frac{1}{Bi_{gs,A}} \geq 0 \quad (8)$$

$$\frac{1}{\delta\gamma} + 1 - C_{AL} \frac{\frac{1}{\phi_A} + \frac{1}{Bi_{Ls,B}}}{\frac{1}{\phi_A} + \frac{1}{Bi_{Ls,A}}}$$

If ω from Eq. 8 is evaluated to be less than zero, it is set equal to zero everywhere. When ω is equal to zero, there are still no limitations imposed by the nonvolatile zero-order reactant B . However if ω from Eq. 8 is greater than zero, the overall effectiveness factor for this dry-wet pellet shows a dependence upon the flowing liquid concentration of the nonvolatile reactant. One can show that under such conditions ($\omega > 0$), the expression for the effectiveness factor can be represented by $\eta_{odw} = C_1 + C_2 C'_{BL}$, where C_1 and C_2 are constants. Once ω has been determined, $\tanh[\phi_A(1 - \omega)]$ must be checked to make sure that it is approximately 1.0, i.e., $\phi_A(1 - \omega) > 3$. If it is not, then ω must be determined from a more complex set of equations shown in the Appendix.

Large ϕ_A solution for $m < 1$

The overall effectiveness factor for a reaction of order less than one on the dry-wet pellet is found by substituting the reactant profiles for C_A given in the Appendix into Eq. 6. The overall effectiveness factor is then given by:

$$\eta_{odw} = \frac{1}{2} \left(\frac{1 - m}{1 + m} \right)^{(1+m)/(1-m)} \phi_A^{2m/(1-m)} \cdot [(1 - \omega_x - \omega)^{(1+m)/(1-m)} + (1 - \omega_y)^{(1+m)/(1-m)}] \quad (9)$$

The value of ω_y is found by solving Eq. T1.1 of Table 1 and the values of ω and ω_x are found by simultaneously solving Eq. T1.2 and T1.3. To solve Eqs. T1.1–T1.3 for the ω 's, it is helpful to place upper and lower bounds on them. The value of ω is bounded by zero and the value obtained from Eq. T1.2 when ω_x is zero. The values of $(\omega_x + \omega)$ and ω_y are both bounded by the expression $(1 + m)/[(1 - m)\phi_A]$ and one. When the righthand side of Eq. T1.3 evaluates to greater than zero, then ω equals zero and the nonvolatile zero-order reactant does not influence the reaction rate since its concentration is nonzero throughout the pellet including the dry surface ($C_{B0} > 0$).

Reactor-scale Overall Effectiveness Factor

The infinite-slab geometry, where a face can only be actively wetted or inactively wetted, can only be used to derive particle-scale overall effectiveness factors for completely inactively wetted slabs (η_{od}), half-wetted slabs (η_{odw} , derived in the previous section), and fully actively wetted slabs (η_{ow}). There would be no reaction occurring on a pellet that was completely externally dry because the nonvolatile reactant B could not be supplied to the catalyst; therefore, $\eta_{od} = 0$. If the pellet were actively wetted on both sides, then the overall effectiveness factor for this wetted

pellet would be, for $m = 1$:

$$\eta_{ow} = \frac{1}{\phi_A^2} \left[\frac{C_{AL}}{\frac{1}{\phi_A \tanh(\phi_A)} + \frac{1}{Bi_{Ls,A}}} \right] \quad (10)$$

where $\tanh(\phi_A) = 1$ for large ϕ_A . For $m < 1$, the overall effectiveness factor for a completely externally wetted pellet, valid for large ϕ_A , is:

$$\eta_{ow} = \left(\frac{1 - m}{1 + m} \right)^{(1+m)/(1-m)} \phi_A^{2m/(1-m)} (1 - \omega_y)^{(1+m)/(1-m)} \quad (11)$$

where ω_y is the solution to Eq. T1.1.

The completely inactively wetted, half-wetted, and completely actively wetted slabs would have external wetting (or contacting) efficiencies of 0.0, 0.5, and 1.0, respectively. To obtain an overall effectiveness factor for any value of the contacting efficiency η_{ce} , the bed fractions represented by these slabs must be appropriately weighted.

The simplest weighting of slabs is to assume that a slab face can only be wet or dry. Since the contacting efficiency η_{ce} is the fraction of external catalyst surface area that is actively wetted, η_{ce} is equal to the probability that a slab face is actively wetted. The probability that a slab face is dry (inactively wetted) would then be $1 - \eta_{ce}$.

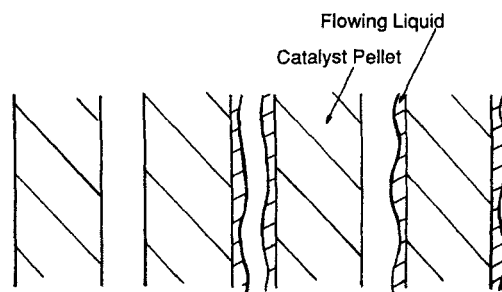
The fraction of particles in the bed that would be completely externally dry (inactively wetted) is $(1 - \eta_{ce})^2$, half-wetted is $2\eta_{ce}(1 - \eta_{ce})$, and completely actively wetted is η_{ce}^2 , as shown in Figure 4. A reactor-scale overall effectiveness factor η_o valid for any contacting efficiency can be defined simply as the sum of the product of the fraction of particles in a certain group and the overall effectiveness factor for that group:

$$\eta_o = (1 - \eta_{ce})^2 \eta_{od} + 2(1 - \eta_{ce})\eta_{ce}\eta_{odw} + \eta_{ce}^2 \eta_{ow} \quad (12)$$

The above definition of the reactor-scale overall effectiveness factor only implies good radial mixing in an integral trickle-bed reactor.

Large ϕ_A solution for $m = 1$

The overall reactor-scale effectiveness factor for a first-order



Volume Fraction of Packing:

$$(1 - \eta_{ce})^2 + \eta_{ce}(1 - \eta_{ce}) + \eta_{ce}(1 - \eta_{ce}) + \eta_{ce}^2 = 1.0$$

Figure 4. Weighting of slabs for reactor-scale overall effectiveness factor.

reaction with a large Thiele modulus ($\phi_A > 4$) is found by substituting Eq. 7 and 10 into Eq. 12.

$$\eta_o = \frac{1}{\phi_A^2} \left[\frac{\eta_{ce} C_{AL}}{\frac{1}{\phi_A} + \frac{1}{Bi_{Ls,A}}} + \frac{\eta_{ce} (1 - \eta_{ce})}{\omega + \frac{1}{\phi_A} + \frac{1}{Bi_{gs,A}}} \right] \quad (13)$$

where ω is given by Eq. 8.

Large ϕ_A solution for $m < 1$

The overall reactor-scale effectiveness factor for a less than first-order reaction with a large Thiele modulus [$\phi_A > (1 + m)/(1 - m)$] is found by substituting Eq. 9 and 11 into Eq. 12.

$$\eta_o = \left(\frac{1 - m}{1 + m} \right)^{(1+m)/(1-m)} \cdot \phi_A^{2m/(1-m)} [\eta_{ce}(1 - \eta_{ce})(1 - \omega_x - \omega)^{(1+m)/(1-m)} + \eta_{ce}(1 - \omega_y)^{(1+m)/(1-m)}] \quad (14)$$

where, as described above, ω_y is found by solving Eq. T1.1 and the values of ω and ω_x are found by simultaneously solving Eqs. T1.2 and T1.3 of Table 1. As stated previously, if C_{AL} is approximately constant, then in all of the above expressions C_{AL} can be replaced by one and $Bi_{Ls,A}$ by $Bi_{gLs,A}$ defined in Eq. 5.

Reactant B Conversion

The apparent reaction rate of the nonvolatile zero-order reactant B per unit reactor volume r_{av} at any axial position is given by:

$$r_{av} = b(1 - \epsilon) \frac{V_s}{V_p} k_{vs} \eta_o (C_A^*)^m \quad (15)$$

where η_o is given by Eq. 13 for $m = 1$ and by Eq. 14 for $m < 1$. This is also the rate that would be observed in a partially wetted trickle-bed reactor with differential conversions per pass.

If the liquid in the trickle-bed reactor is assumed to be in plug flow, the following dimensionless differential equation arises for the conversion of the nonvolatile reactant X_B in the flowing liquid:

$$\frac{dX_B}{dz} = Da \gamma_i \eta_o \quad (16)$$

where:

$$Da = k_{vs} (C_A^*)^{m-1} \frac{V_s L_r}{V_p u_L} (1 - \epsilon)$$

$$\gamma_i = bC_A^*/C_{Bi} \quad z = z'/L_r$$

Da is a modified Damkohler number with L_r and u_L being the packed bed length and the superficial liquid velocity, respectively. The dimensional and dimensionless packed bed axial coordinates are z' and z , respectively. C_{Bi} is the dimensional inlet concentration of the reactant B. The overall effectiveness factor η_o is given by Eq. 13 for $m = 1$ and by Eq. 14 for $m < 1$. The initial condition for this equation is at $z = 0$, $X_B = 0$.

The differential equation for the outlet conversion of the nonvolatile reactant can be solved analytically when the following assumptions are satisfied (in addition to those listed for the particle model):

1. The reaction is first order in the volatile reactant A ($m = 1$).
2. The reactor is isothermal and at steady state.
3. The concentration of reactant A in the gas phase changes very little.

Table 1. Equations for Evaluation of ω_x , ω_y , and ω or C_{B0} for $m < 1$ on Half-wetted Slab

Valid for $\phi_A > (m + 1)/(m - 1)$

1. Find ω_y by solving:

$$0 = \frac{1 + m}{1 - m} \left[\left(1 - \omega_y + \frac{2}{Bi_{Ls,A}(1 - m)} \right) / C_{AL} \right]^{(m-1)/2} - \phi_A (1 - \omega_y)^{(m+1)/2} \quad (T1.1)$$

2. First, try $\omega = 0$. Solve the following two equations for ω_x and C_{B0} . If C_{B0} is found to be greater than zero, then $\omega = 0$; otherwise, $C_{B0} = 0$, and re-solve the following two equations for ω_x and ω :

$$0 = \frac{1 + m}{1 - m} \left[1 - \omega_x - \omega + \left(\omega + \frac{1}{Bi_{gs,A}} \right) \frac{2}{1 - m} \right]^{(m-1)/2} - \phi_A (1 - \omega_x - \omega)^{(m+1)/2} \quad (T1.2)$$

$$\begin{aligned} \text{For } C_{B0} = 0, 0 \\ \text{For } \omega = 0, C_{B0} \Bigg\} &= 1 - \delta \gamma \left(\frac{1 - m}{1 + m} \right)^{(1+m)/(1-m)} \phi_A^{2/(1-m)} \left\{ (1 - \omega_x - \omega)^{2/(1-m)} \right. \\ &\quad + (1 - \omega_x - \omega)^{(1+m)/(1-m)} \left[2 \left(\frac{V_p}{V_s} - 1 \right) + \omega_y + \omega_x \right] \frac{2}{1 + m} \\ &\quad + \frac{1 - m}{1 + m} (1 - \omega_y)^{2/(1-m)} + \frac{2}{1 + m} (1 - \omega_y)(1 - \omega_x - \omega)^{(1+m)/(1-m)} \Bigg\} \\ &\quad - \frac{2\delta\gamma}{Bi_{Ls,B}(1 + m)} \left(\frac{1 - m}{1 + m} \right)^{(1+m)/(1-m)} \phi_A^{2/(1-m)} [(1 - \omega_y)^{(1+m)/(1-m)} \\ &\quad + (1 - \omega_x - \omega)^{(1+m)/(1-m)}] \end{aligned} \quad (T1.3)$$

4. The concentration of reactant A dissolved in the liquid phase changes very little, so that C_{AL} can be replaced by unity and $Bi_{L,A}$ by $Bi_{g,L,A}$. This is considered valid for a slightly soluble gas.

5. The liquid is in plug flow.

6. Liquid physical properties are considered constant throughout the packed bed. This is valid if the liquid consists mainly of a solvent, if the conversion of the nonvolatile reactant is small, or if the physical properties of the nonvolatile product are similar to those of the nonvolatile reactant.

Table 2 presents equations for the outlet conversions of the nonvolatile zero-order reactant B when the assumptions detailed above and those given for the half-wetted particle model hold.

Comparison of Model Predictions and Data

α -Methylstyrene hydrogenation

To obtain model predictions for the hydrogenation of α -methylstyrene in n -hexane over a 5 wt. % palladium-on-alumina catalyst (Mills et al., 1984), several values had to be estimated or measured. The intrinsic kinetics in n -hexane solvent reported by El-Hisnawi et al. (1982) were extrapolated to get k_{vs} for the 5% catalyst, which was assumed to have a uniform metal content. Apparent kinetics with no external mass transfer resistances were measured in the stirred-basket reactor discussed by El-Hisnawi et al. to obtain the catalytic effectiveness factor η .

The effective diffusivity of hydrogen D_{eA} was calculated from the extrapolated intrinsic and measured apparent kinetics ($\eta =$

$1/\phi_A$ for large ϕ_A). The solubility of hydrogen in α -methylstyrene was estimated from the correlation of Herskowitz et al. (1978) and in n -hexane or cyclohexane from the Wilhelm and Battino (1973) review. The molecular diffusivities of hydrogen and α -methylstyrene in the liquid were estimated from the correlation of Akgerman and Gainer (1972) and correlations given in Reid et al. (1977), respectively. The ratio of the effective diffusivities (δ) was assumed equal to the ratio of the molecular diffusivities. Most liquid and gas physical properties, vapor pressure values, and required mixing rules were obtained from Reid et al. (1977), and the liquid and vapor were assumed to be in equilibrium at the top of the catalyst bed.

The correlations used for wetting efficiency and mass transfer coefficients are given in Table 3. These correlations were chosen because they gave the best prediction of the column's performance at high liquid velocities for the 5% catalyst, when analyzed by Mills et al. (1984) using a model considering the intrapellet mass balance of the hydrogen only. At high liquid velocities the bed is completely wetted and because of the high catalyst activity the external mass transfer resistance for the gas reactant is dominant in controlling the rate. It is noteworthy that in order to achieve a good match with data in completely wetted beds, the gas-to-liquid mass transfer coefficient at the actively wetted surface $(Ka)_{g,L,A}$ was assumed infinite, although the correlation of Fukushima and Kusaka (1977) would indicate that it is only approximately 60% of the liquid-to-solid mass transfer rate.

A plot of model-predicted conversion and experimentally

Table 2. Reactor Outlet Conversions for $m = 1$ and Large ϕ_A

Valid when liquid- and gas-phase compositions of the first-order reactant A are constant, the liquid is in plug flow, the reactor is isothermal, physical and transport properties are constant, and the Thiele modulus is large ($\phi_A > 4$).

1. Calculate the outlet conversion of the zero-order nonvolatile reactant B , if there were no B limitations on the half-wetted pellet:

$$X_{B1} = \frac{\gamma_i Da}{\phi_A^2} \left[\frac{\eta_{ce}}{\frac{1}{\phi_A} + \frac{1}{Bi_{g,L,A}}} + \frac{(1 - \eta_{ce})\eta_{ce}}{\frac{1}{\phi_A} + \frac{1}{Bi_{g,S,A}}} \right] \quad (T2.1)$$

2. Calculate the conversion at which nonvolatile reactant B limitations begin, X_{Bc} (if less than zero, set equal to zero):

$$X_{Bc} = 1 - \gamma_i \delta \left(\frac{2 \frac{V_p}{V_s} + \frac{1}{Bi_{L,S,B}} + \frac{1}{Bi_{g,S,A}}}{\frac{1}{\phi_A} + \frac{1}{Bi_{g,S,A}}} + \frac{\frac{1}{Bi_{L,S,B}} - \frac{1}{Bi_{g,L,A}}}{\frac{1}{\phi_A} + \frac{1}{Bi_{g,L,A}}} \right) \geq 0 \quad (T2.2)$$

3. Calculate X_B , the reactor outlet conversion:

If $X_{B1} \leq X_{Bc}$ or $\eta_{ce} = 1$, then $X_B = X_{B1}$. Otherwise,

$$X_B = 1 + X_{Bw} - (1 - X_{Bc} + X_{Bw})e^{[-X_{Bd}(1 - X_{Bc}/X_{B1})]} \quad (T2.3)$$

where:

$$X_{Bw} = \frac{\delta \gamma_i}{\frac{1}{\phi_A} + \frac{1}{Bi_{g,L,A}}} \left[\frac{1}{Bi_{g,L,A}} + \left(2 \frac{V_p}{V_s} + \frac{1}{Bi_{g,S,A}} + \frac{\eta_{ce}}{Bi_{L,S,B}} \right) \frac{1}{1 - \eta_{ce}} \right]$$

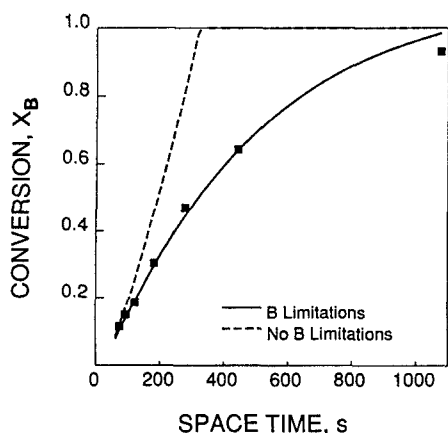
$$X_{Bd} = \frac{Da(1 - \eta_{ce})\eta_{ce}}{\delta \phi_A^2 \left(2 \frac{V_p}{V_s} + \frac{1}{Bi_{L,S,B}} + \frac{1}{Bi_{g,S,A}} \right)}$$

Table 3. Correlations Used in Model

Correlation	Reference
$\eta_{ce} = 1.617 Re_L^{0.146} Ga_L^{-0.0711} \leq 1$	El-Hisnawi et al. (1982)
$k_{Ls} = 4.25 \frac{D_m \epsilon_p}{d_p \eta_{ce}} Re_L^{0.48} Sc_L^{0.33}$	Tan and Smith (1982)
$k_{gA} = 0.4548 \frac{H_A u_g}{\epsilon} Re_g'^{-0.4069} Sc_g'^{-0.667}$	Dwivedi and Upadhyah (1977)
$(Ka)_{gLA} \rightarrow \infty$	

measured conversion (Mills et al., 1984) of α -methylstyrene in *n*-hexane over a 0.21 m length of 5 wt. % palladium-on-alumina catalyst vs. reactor liquid space time (L_r/u_L) from 50 to 1,100 s is shown in Figure 5. The model used is given in Table 2, with the correlations given in Table 3 and the property estimates in Table 4. The model predicts the correct trends, and the predictions are very accurate. This is remarkable considering that the model uses independently determined kinetic and diffusion parameters and mass transfer correlations that fit the data only at very low space times. The model's ability to correctly and quantitatively predict the trend of data indicates that it is based on the correct description of physical phenomena. Figure 5 also contains model predictions, shown by the dashed line, using the mass transfer and wetting efficiency correlations given in Table 3, but neglecting the limitations of the *B* reactant as had been done previously in attempts to fit this data (Mills et al., 1984) and as had been advocated by other investigators.

Model predictions are compared in Figures 6–9 to the experimentally measured conversions (El-Hisnawi, 1981; El-Hisnawi et al., 1982; Mills and Duduković, 1984) for the α -methylstyrene hydrogenation in *n*-hexane or cyclohexane solvents over 2.5 or 0.5 wt. % palladium-on-alumina external shell catalysts. The packing length was 0.40 m and the reactor pressure was assumed to be 1.04×10^5 Pa, which was the system pressure when the 5% catalyst was used. The wrong pressure of 2.4×10^5 Pa had been recorded for the work of El-Hisnawi (1981). For all the data, the predictions are excellent when using the models in

Figure 5. α -Methylstyrene conversion on 5% catalyst and *n*-hexane solvent.

■ Exp. data; ——— Model predictions for data of Mills et al. (1984)

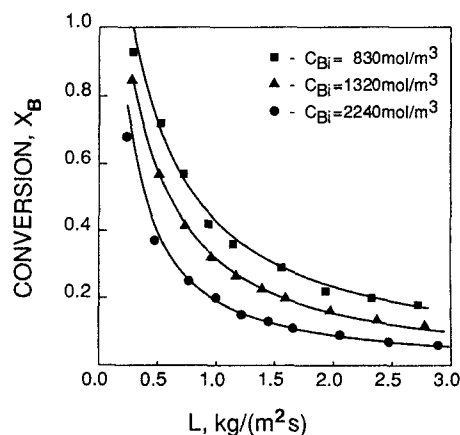
Table 4. Property Estimates Used in Model

Property	Figure 5 Lower Curve	Figure 10 Lowest Curve
m	1.00×10^0	6.00×10^{-1}
V_t, m^3	6.84×10^{-9}	2.90×10^{-8}
V_p, m^3	6.84×10^{-9}	2.90×10^{-8}
S_x, m^2	2.11×10^{-5}	5.23×10^{-5}
$k_{ws}, (mol/m^3)^{1-m}/s$	4.97×10^2	5.14×10^0
η	1.95×10^{-2}	7.59×10^{-2}
$C_A^*, mol/m^3$	3.76×10^0	1.00×10^0
H_A	9.82×10^0	5.22×10^1
$C_{g1}, mol/m^3$	1.71×10^3	2.00×10^1
L_r, m	2.11×10^{-1}	—
$\rho_L, kg/m^3$	7.23×10^2	9.94×10^2
$\mu_L, kg/m \cdot s$	3.69×10^{-4}	6.48×10^{-4}
$D_{mA}, m^2/s$	1.51×10^{-8}	7.60×10^{-9}
$D_{mB}, m^2/s$	3.07×10^{-9}	1.84×10^{-9}
ϵ	5.27×10^{-1}	5.00×10^{-1}
ϵ_p	8.03×10^{-1}	5.37×10^{-1}
$\rho_g, kg/m^3$	5.63×10^{-1}	1.45×10^{-1}
$\mu_g, kg/m \cdot s$	9.36×10^{-6}	9.89×10^{-6}
$u_g, m/s$	3.98×10^{-2}	3.79×10^{-3}
$D_{mGA}, m^2/s$	3.10×10^{-5}	6.21×10^{-5}

Table 2 and the correlations in Table 3. The largest deviation occurs in Figure 7 at higher liquid flows for the *n*-hexane solvent over the 2.5% palladium-on-alumina catalyst. This points to the possible inadequacy of the mass transfer correlation used. This is a perennial problem with empirical correlations, that good results are not obtained in all systems. Figure 9 also contains model predictions, shown by the dashed line, using the mass transfer and wetting efficiency correlations given in Table 3, but neglecting the limitations of the *B* reactant as shown previously (El-Hisnawi, 1981; El-Hisnawi et al., 1982; Mills and Duduković, 1984). The reduction in conversion due to the nonvolatile zero-order reactant *B* varies between the runs and is the largest in Figure 9.

Maleic acid hydrogenation

To model the differential reactor of Ruiz et al. (1984) for the hydrogenation of maleic acid to succinic acid in water, the same

Figure 6. α -Methylstyrene conversion on 0.5% catalyst and *n*-hexane solvent.

■▲● Exp. data; ——— Model predictions for data of El-Hisnawi (1981)

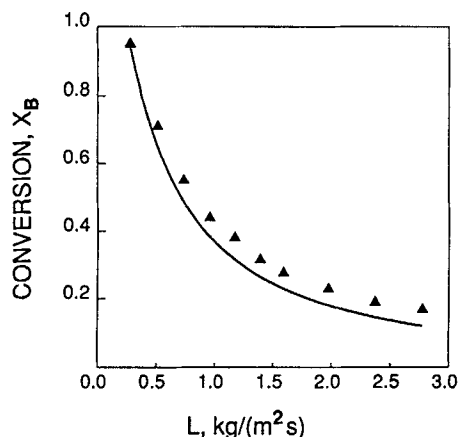


Figure 7. α -Methylstyrene conversion on 2.5% catalyst and *n*-hexane solvent.

▲ Exp. data; — Model predictions for data of El-Hisnawi et al. (1982)

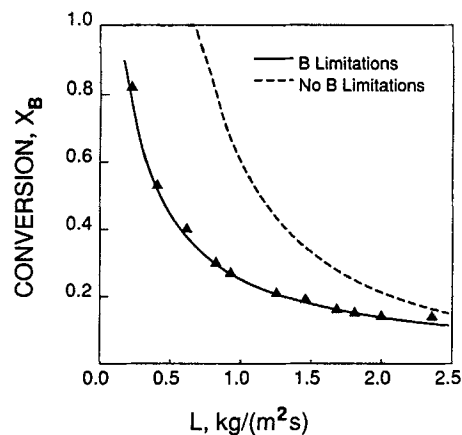


Figure 9. α -Methylstyrene conversion on 2.5% catalyst and cyclohexane solvent.

▲ Exp. data; --- Model predictions for data of El-Hisnawi et al. (1982)

mass transfer and wetting efficiency correlations were used as in the α -methylstyrene system, given in Table 3. The kinetic equations, catalyst properties, and experimental parameters were given by Ruiz et al. The metal in the catalyst was assumed to be uniformly dispersed and the intrinsic kinetics were assumed to be independent of the metal dispersion. The bed porosity was assumed to be 0.5. Physical properties were estimated using the same correlations and methods as for the hydrogenation of α -methylstyrene. An equilibrium relation for hydrogen dissolved in water was estimated from the data of Morrison and Billett (1952). The properties used are given in Table 4 for the lowest curve in Figure 10.

A plot of the data of Ruiz et al. compared to the model predictions from Eqs. 15 and 14 and Table 1 is shown in Figure 10. The plot is of reaction rate r_{av} in moles of maleic acid consumed/ m^3 reactor $\cdot s$ vs. liquid mass superficial velocity in $kg/m^2 \cdot s$ as the inlet concentration of maleic acid is varied from 215 mol/ m^3 down to 20 mol/ m^3 at 308 K and 1.4×10^5 Pa. The model does a satisfactory job of predicting the trend of the data as the inlet maleic acid concentration is changed. Only at the highest con-

centration does the maleic acid not limit the reaction rate. Previous models have been unable to predict the significant reduction in reaction rate with the decrease in the inlet maleic acid concentration.

Discussion

Using the correlations in Table 3 and the model in Table 2, the outlet conversions of α -methylstyrene for the data of El-Hisnawi (1981) and Mills et al. (1984) are predicted accurately in Figures 5–9. The largest deviations occur at the higher liquid flows for *n*-hexane solvent over the 2.5 wt. % palladium-on-alumina catalyst in Figure 7. This is the first time that these data have been successfully modeled based on the assumption that the inactively wetted surfaces are dry and provide a negligible mass transfer resistance for the hydrogen. This had been the standard assumption used by several workers in modeling the α -methylstyrene hydrogenation under different conditions (Herskowitz et al., 1979; Morita and Smith, 1978; Tan and Smith, 1980; Sakornwimon and Sylvester, 1982; Capra et al., 1982; Ramachandran and Smith, 1979).

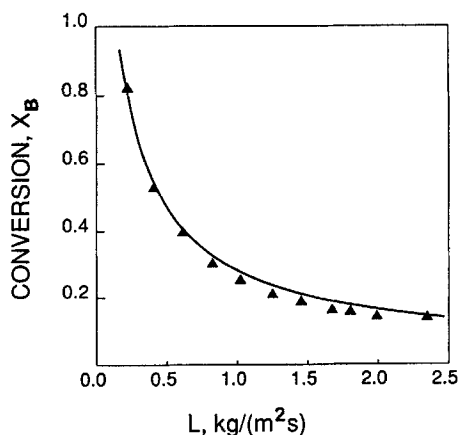


Figure 8. α -Methylstyrene conversion on 0.5% catalyst and cyclohexane solvent.

▲ Exp. data; — Model predictions for data of El-Hisnawi et al. (1982)

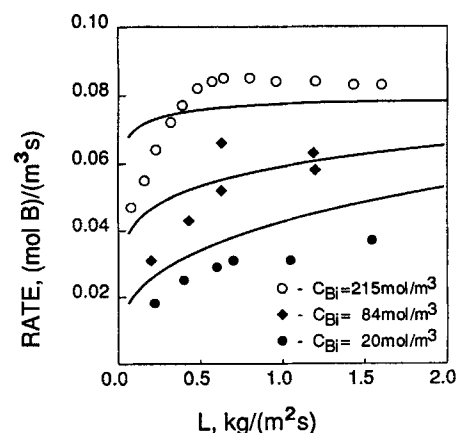


Figure 10. Maleic acid conversion in water.

○ ● Exp. data; — Model predictions for data of Ruiz et al. (1984)

An examination of Eq. 13 shows why previous attempts to model the diluted α -methylstyrene hydrogenation required a finite resistance at the inactively wetted surface (El-Hisnawi, 1981; El-Hisnawi et al., 1982; Mills and Duduković, 1984; Mills et al., 1984). The contribution to the reaction rate occurring near the inactively wetted surfaces contains an additional resistance ω , which is due to the layer of liquid in the pores through which the hydrogen must diffuse before it encounters any α -methylstyrene for reaction. This resistance had been attributed to a significant mass transfer resistance at the inactively wetted surface, $1/Bi_{gs,A}$. The effect due to the nonvolatile zero-order α -methylstyrene varies greatly in the different runs, explaining the marginal success in fitting the data previously when assuming a constant mass transfer resistance at the inactively wetted surfaces. This is also the reason why the previous model with two resistances (Mills and Duduković, 1984) could not be used to predict the results for catalysts of different activities. The current model shows complete predictability with respect to catalyst activity, catalyst type (shell vs. uniform), and level of liquid reactant concentration.

The proper trends for the data of Ruiz et al. (1984) as the inlet maleic acid content is changed, shown in Figure 10, are predicted using the correlations in Table 3 and the rate of reaction obtained from Eq. 15 with Eq. 14 and Table 1. The apparent and intrinsic kinetics had been measured to be of 0.06 and 0.08 order, respectively, in the maleic acid concentration (Ruiz et al.), but were modeled here to be to the zero order. Previous models, neglecting the distribution of the nonvolatile maleic acid reactant in the pellet, would predict at most a 13% reduction in the observed rate as the maleic acid concentration is reduced from 215 to 20 mol/m³. The correct prediction by this model of a much greater reduction, up to 70%, is in much better agreement with the data and is an independent confirmation of the validity of the effects due to the nonvolatile reactant being depleted near the inactively wetted surfaces of partially wetted pellets.

Some comments are necessary concerning the correlations shown in Table 3. There is no correlation available for estimating the mass transfer coefficient from the gas to the inactively wetted or dry surfaces, $k_{gs,A}$. The correlation of Dwivedi and Upadhyah (1977) for the evaporation of liquid from solid particles was used as an estimate. This correlation predicts very large mass-transfer coefficients, so that the term $1/Bi_{gs,A}$ is negligible in each case and the physical properties of the gases given in Table 4 were not actually needed.

The wetting efficiency correlation of El-Hisnawi et al. (1982), upon which our model relies, was obtained from nonadsorbing impulse tracer studies in trickle-bed reactors containing porous packings. The correlation should be adequate for systems near room temperature and atmospheric pressure with negligible heat effects.

The overall mass transfer coefficient from the gas to the flowing liquid, $(Ka)_{gL,A}$, was assumed to be infinite to predict the conversions of α -methylstyrene over the 5% palladium-on-alumina catalyst at the higher liquid flow rates. This does not necessarily mean that $(Ka)_{gL,A}$ is large. Actually, the overall mass transfer coefficient from the gas to the actively wetted solid was assumed to be given by the liquid-to-solid correlation of Tan and Smith (1982), which is approximately 2.5 times the overall mass transfer coefficient obtained from Eq. 5 using the correlation of Fukushima and Kusaka (1977) for $(Ka)_{gL,A}$ and of Tan and

Smith (1982) for $k_{Ls,A}$. If the overall mass transfer coefficient from the gas to the actively wetted solid is 40% less, then the η_{ce} correlation would have to be reduced about 0.1 to obtain the measured conversions.

Some observations can be made about the model. As the wetting efficiency becomes complete ($\eta_{ce} = 1$), the nonvolatile zero-order reactant will not limit the reaction rate in a trickle-bed reactor unless the product of the diffusivity and concentration ratios of reactant B to A is less than one. When η_{ce} is less than one, Eq. T2.2 is important because it gives the conversion at which B begins to limit the reaction for a first-order reaction rate. An approximate criterion can be established from Eq. T2.2 for this critical conversion, X_{Bc} , for a uniformly dispersed catalyst ($V_p = V_s$) and a large Thiele modulus. Approximating the mass-transfer resistance at the dry surface to be zero ($1/Bi_{gs,A} \approx 0$) and the Biot numbers at the actively wetted surface to be approximately one ($Bi_{Ls,B} \approx Bi_{gL,A} \approx 1$), then:

$$X_{Bc} = 1 - \frac{3 \phi_A b C_A^* D_{eA}}{C_{Bi} D_{eB}} \quad (17)$$

If the reaction in a partially wetted trickle-bed reactor is first order in gas reactant A , then the reaction rate may be decreased if conversion exceeds X_{Bc} .

Viewing the slabs as individual particles implies that the particles in the bed can be divided into three groups: approximately completely externally wetted, half-wetted externally, and completely inactively wetted or externally dry. Intuitively, this approaches reality better than the assumption that all particles have the same fraction of external wetting. If the zero-order reactant B had been significantly volatile so that it was accessible to all particles, the model in this paper would be identical to the approximate overall effectiveness factor for slab geometry and large ϕ_A used previously (Mills and Duduković, 1984; Mills et al., 1984). In the case of nonvolatile B , since the model involves solving differential equations in only one dimension, the model should be useful for the numerical solution of Langmuir-Hinshelwood kinetics in partially wetted pellets.

Conclusions

In trickle-bed reactors at low liquid mass velocities ($L < 5 \text{ kg/m}^2 \cdot \text{s}$) when catalyst particles are incompletely wetted, a nonvolatile zero-order liquid reactant may affect the reaction rate. This occurs even when $D_{eB} C'_{B0}/D_{eA} C_A^* \gg 1$, which is the condition that guarantees no liquid reactant effects in completely wetted particles. The effect can be expected when the liquid reactant conversion exceeds the critical value of $1 - 3 \phi_A D_{eA} b C_A^*/D_{eB} C_{Bi}$. It is caused by the inability of the liquid reactant to diffuse rapidly enough to the zones adjacent to the dry catalyst surface where the gas reactant is abundant. This leads to formation of an inactive catalyst zone where liquid reactant is completely depleted. A single-particle model illustrates this effect. The bed model consists of an assembly of externally dry, half-wetted, and completely wetted particles, the ratios of which are determined by the catalyst contacting efficiency. Using independently measured kinetic parameters and transport coefficients, the model predicts well the results in two experimental systems. The model's ability to correctly predict the experimental results is unaffected by catalyst activity, type (shell vs. uniform catalyst), or liquid carrier used (hexane, cyclohexane, water). It is noteworthy

thy that the model worked well with the assumption that the mass transfer resistance for the gas at the dry surface is negligible, supporting the assumption made by several workers (Morita and Smith, 1978; Herskowitz et al., 1979).

Acknowledgment

Support from the industrial participants in the Chemical Reaction Engineering Laboratory (CREL) made this work possible.

Notation

A = gaseous reactant (hydrogen)
 b = stoichiometric coefficient for B
 B = nonvolatile liquid reactant (α -methylstyrene or maleic acid)
 Bi = Biot number = kV_s/D_eS_x
 c, d, f, g, p, q, r, s = integration constants, Table A1
 C = reactant concentration
 C' = reactant concentration, mol/m³ liquid
 C_A^* = dissolved gas concentration in equilibrium with bulk gas concentration, mol/m³ liquid
 C_{Bi} = bulk B liquid inlet concentration, mol/m³ liquid
 C_{B0} = B concentration at inactive wetted surface
 d_p = pellet diameter = $6V_p/S_x$, m
 D_e = effective diffusivity in pellet, m³ liquid/m pellet · s
 D_m = molecular diffusivity, m²/s
 Da = Damkohler number = $k_{rs}(C_A^*)^{m-1}V_sL_r(1-\epsilon)/(V_pu_L)$
 g = gravity acceleration, m/s²
 Ga = Galileo number = $gd_p^3\rho_L^2/\mu_L^2$
 H = Henry's law constant, m³ liquid/m³ gas
 k = mass transfer coefficient based on liquid concentration, m³ liquid/m² external area · s
 k_{rs} = m th-order reaction rate constant based on volume of catalyst shell, (mol A)^{1-m} · (m³ liquid) ^{m} /m³ external shell · s
 $(Ka)_{gL,A}$ = overall volumetric mass transfer coefficient from gas to flowing liquid for A based on dissolved concentration, m³ liquid/m³ empty reactor · s
 L = liquid mass velocity, kg/m² empty reactor · s
 L_r = length of packed bed, m
 m = reaction order with respect to reactant A
 r_{av} = apparent reaction rate, mol B /m³ empty reactor · s
 Re = Reynolds number = $d_p u \rho / \mu$
 Re' = Reynolds number = $(S_x/\pi)^{0.5} u \rho / \mu$
 S_x = external surface area of a catalyst pellet, m²
 Sc = Schmidt number = $\mu/\rho D_m$
 u = superficial velocity, m³ fluid/m² empty reactor · s
 V_p = volume of a catalyst pellet, m³
 V_s = volume of external shell in a catalyst pellet, m³
 x = coordinate in external shell to inactive wetted surface or plane where B is depleted = $1 - [x' - \omega V_i/S_x]/[(1 - \omega_x - \omega) V_i/S_x]$
 x' = coordinate in pellet slab from inactive wetted surface to active wetted surface, m
 X_B = conversion of reactant B
 X_{B1} = reactor outlet conversion of B for a first-order reaction when B does not limit the reaction rate
 X_{Bc} = critical conversion of reactant B above which B limits the reaction rate
 X_{Bd}, X_{Bw} = terms defined in Table 2
 y = coordinate in external shell to active wetted surface = $[x' - 2V_p/S_x + (1 - \omega_y) V_i/S_x]/[(1 - \omega_y) V_i/S_x]$
 z = reactor coordinate from top = z'/L_r
 z' = reactor coordinate from top of packing, m

Greek letters

γ = concentration ratio in bulk liquid = bC_A^*/C_{BL}
 γ_i = concentration ratio at reactor inlet = bC_A^*/C_{Bi}

δ = ratio of effective diffusivities = D_{eA}/D_{eB}
 ϵ = bed porosity, m³ external voids/m³ empty reactor
 ϵ_p = pellet porosity, m³ pores/m³ pellet
 η = catalyst effectiveness factor measured in a stirred-basket reactor with negligible external mass transfer resistance
 η_{ce} = external contacting or wetting efficiency based on total external surface area
 η_o = overall pellet effectiveness factor based on total amount of catalyst metal and bulk concentration of C_A^*
 μ = viscosity, kg/m · s
 ρ = density, kg/m³
 ϕ_A = generalized Thiele modulus = $(V_i/S_x)\{[(m+1) \cdot k_{rs}(C_A^*)^{m-1}]/2D_{eA}\}^{0.5}$
 ω = twice the fraction of catalyst where no reaction is occurring because no reactant B is present in a half-wet pellet
 ω_x = fraction of catalyst shell near an inactive wetted surface where no reaction occurs because A has been depleted = 0 when $m = 1$
 ω_y = fraction of catalyst shell near an active wetted surface where no reaction occurs because A has been depleted = 0 when $m = 1$

Subscripts

A = reactant A
 B = reactant B
 d = with two externally dry faces of slab
 $d\omega$ = with an inactive and active wetted face
 g = gas phase
 gs = from gas to inactive wetted solid
 gLs = from gas to active wetted solid
 L = flowing liquid
 Ls = from liquid to active wetted solid
 w = with two active wetted faces of slab

Appendix

Reactant profiles for $m = 1$ (any ϕ_A)

The solutions to the differential equations, Eqs. 1–4, obviously depend upon the value of m . When the intrinsic kinetics are first order in the gas reactant A ($m = 1$), the solution is analytical and both ω_x and ω_y are zero since the gas reactant cannot be fully consumed. The solutions for the reactant profiles within the catalyst pellet follow for $m = 1$. For $0 < x < 1$,

$$C_A = c \cosh [\phi_A(1 - \omega)x] + d \sinh [\phi_A(1 - \omega)x] \quad (A1)$$

$$C_B = \delta \gamma \{c \cosh [\phi_A(1 - \omega)x] + d \sinh [\phi_A(1 - \omega)x] + fx + g\} \quad (A2)$$

For $0 < y < 1$,

$$C_A = p \cosh (\phi_A y) + q \sinh (\phi_A y) \quad (A3)$$

$$C_B = \delta \gamma [p \cosh (\phi_A y) + q \sinh (\phi_A y) + ry + s] \quad (A4)$$

The nine equations, A1.1–A1.9, that must be solved for ω and the eight integration constants are given in Table A1. The righthand side of Eq. A1.9 is $C_{B0}/(\delta \gamma)$, where C_{B0} is the dimensionless concentration of reactant B at $\omega V_i/S_x$ ($x = 1$). To solve the equations in Table A1, the value of ω should first be set equal to zero and if the righthand side of Eq. A1.9 evaluates to greater than zero, then ω is equal to zero and the B reactant is present throughout the catalyst. If the righthand side is less than

Table A1. Equations for Rigorous Evaluation of Integration Constants and ω for $m = 1$ on Half-wetted Slab

First, try $\omega = 0$.

$$d - -q = \frac{\frac{-C_{AL}Bi_{L,A}/\cosh \phi_A}{Bi_{L,A} + \phi_A \tanh \phi_A} + \frac{\{\cosh [\phi_A(1 - \omega)]\}^{-1}}{1 + \left(\phi_A \omega + \frac{\phi_A}{Bi_{g,A}}\right) \tanh [\phi_A(1 - \omega)]}}{\frac{Bi_{L,A} \tanh \phi_A + \phi_A}{Bi_{L,A} + \phi_A \tanh \phi_A} + \frac{\tanh [\phi_A(1 - \omega)] + \phi_A \omega + \frac{\phi_A}{Bi_{g,A}}}{1 + \left(\phi_A \omega + \frac{\phi_A}{Bi_{g,A}}\right) \tanh [\phi_A(1 - \omega)]} + 2\phi_A \left(\frac{V_p}{V_s} - 1\right)} \quad (\text{A1.1-A1.2})$$

$$p = \frac{Bi_{L,A}C_{AL}/\cosh \phi_A + d(Bi_{L,A} \tanh \phi_A + \phi_A)}{\phi_A \tanh \phi_A + Bi_{L,A}} \quad (\text{A1.3})$$

$$c = \frac{\{\cosh [\phi_A(1 - \omega)]\}^{-1} - d\{\tanh [\phi_A(1 - \omega)] + \phi_A \omega + \phi_A/Bi_{g,A}\}}{(\phi_A \omega + \phi_A/Bi_{g,A}) \tanh [\phi_A(1 - \omega)] + 1} \quad (\text{A1.4})$$

$$r = -f/(1 - \omega) = \phi_A \{c \sinh [\phi_A(1 - \omega)] + d \cosh [\phi_A(1 - \omega)]\} \quad (\text{A1.5-A1.6})$$

$$s = d \left(\frac{\phi_A \cosh \phi_A}{Bi_{L,B}} + \sinh \phi_A \right) - p \left(\frac{\phi_A \sinh \phi_A}{Bi_{L,B}} + \cosh \phi_A \right) - r - \frac{r}{Bi_{L,B}} + \frac{1}{\delta \gamma} \quad (\text{A1.7})$$

$$g = s - 2r \left(\frac{V_p}{V_s} - 1 \right) \quad (\text{A1.8})$$

If the righthand side of the following equation is greater than zero when $\omega = 0$, then $\omega = 0$; otherwise, all nine equations must be solved simultaneously with $0 < \omega < 1$.

$$0 = c \cosh [\phi_A(1 - \omega)] + d \sinh [\phi_A(1 - \omega)] + f + g \quad (\text{A1.9})$$

zero, then all nine equations must be solved simultaneously with the constraint that $0 \leq \omega < 1$.

Substituting Eq. A1 and A3 into Eq. 6, the overall effectiveness factor for the dry-wet pellet and a first-order reaction is given as:

$$\eta_{odw} = (c \sinh [\phi_A(1 - \omega)] + d \{\cosh [\phi_A(1 - \omega)] - 1\} + p \sinh (\phi_A) + q [\cosh (\phi_A) - 1]) / (2 \phi_A) \quad (\text{A5})$$

The integration constants c , d , p , and q and the catalyst fraction term ω are obtained by solving the equations in Table A1, as described above. Equations 7 and 8 in the text arise when $\tanh [\phi_A(1 - \omega)]$ and $\tanh (\phi_A)$ are replaced by unity in Table A1 and Eq. A5.

Reactant profiles for $m < 1$ (large ϕ_A)

The reactant profiles within the catalyst particle given below are valid when the reaction is less than first order in the dissolved gas reactant (A) concentration and the generalized Thiele modulus is large enough $[\phi_A > (1 + m)/(1 - m)]$ that the concentration of A within the pellet falls to zero, as shown in Figure 3. The analytical solutions were obtained using the procedure given by Aris (1975), which consists of multiplying Eqs. 1 and 3 by two times the first derivative and integrating with respect to the independent variable twice. For $0 < x < 1$,

$$C_A = \left[(1 - \omega_x - \omega) \phi_A \frac{1 - m}{1 + m} x \right]^{2/(1 - m)} \quad (\text{A6})$$

$$C_B = C_{B0} + \delta \gamma \left\{ (1 - \omega_x - \omega) \phi_A \right\}^{2/(1 - m)} \left(\frac{1 - m}{1 + m} \right)^{(1 + m)/(1 - m)} \cdot \left[1 - \frac{2}{1 + m} x + \frac{1 - m}{1 + m} x^{2/(1 - m)} \right] \quad (\text{A7})$$

For $0 < y < 1$,

$$C_A = \left[(1 - \omega_y) \phi_A \frac{1 - m}{1 + m} y \right]^{2/(1 - m)} \quad (\text{A8})$$

$$C_B = C_{B0} + \delta \gamma \phi_A^{2/(1 - m)} \left(\frac{1 - m}{1 + m} \right)^{(1 + m)/(1 - m)} \left\{ (1 - \omega_x - \omega)^{2/(1 - m)} \cdot \left(1 + \frac{\omega_y + \omega_x}{1 - \omega_x - \omega} \frac{2}{1 + m} \right) + (1 - \omega_y)^{2/(1 - m)} \cdot \left[\frac{1 - m}{1 + m} y^{2/(1 - m)} + \left(\frac{1 - \omega_x - \omega}{1 - \omega_y} \right)^{(1 + m)/(1 - m)} \frac{2}{1 + m} y \right] \right\} \quad (\text{A9})$$

The values for ω_x , ω_y , and ω or C_{B0} are found by solving the equations given in Table 1 and are explained in the text.

Literature Cited

- Akgerman, A., and J. L. Gainer, "Diffusion of Gases in Liquids," *Ind. Eng. Chem. Fundam.*, **11**, 373 (1972).
- Aris, R., *The Mathematical Theory of Diffusion and Reaction in Permeable Catalysts, I: The Theory of the Steady State*, Clarendon, Oxford (1975).
- Capra, V., S. Sicardi, A. Gianetto, and J. M. Smith, "Effect of Liquid Wetting on Catalyst Effectiveness in Trickel-Bed Reactors," *Can. J. Chem. Eng.*, **60**, 282 (1982).

- Duduković, M. P., and P. L. Mills, "Catalyst Effectiveness Factor in Trickle-Bed Reactors," *Chemical Reaction Engineering—Houston*, V. W. Weekman, Jr., and D. Luss, eds., *Am. Chem. Soc. Symp. Ser.*, No. 65, 387 (1978).
- , "Contacting and Hydrodynamics in Trickle-Bed Reactors," *Encyclopedia of Fluid Mechanics*, N. P. Cheremisinoff, ed., Gulf Pub., Houston, Ch. 32, 969–1017 (1986).
- Dwivedi, P. N., and S. N. Upadhyay, "Particle-Fluid Mass Transfer in Fixed and Fluidized Beds," *Ind. Eng. Chem. Process Des. Dev.*, **16**, 157 (1977).
- El-Hisnawi, A. A., "Tracer and Reaction Studies in Trickle-Bed Reactors," D. Sc. Diss., Washington Univ., St. Louis (1981).
- El-Hisnawi, A. A., M. P. Duduković, and P. L. Mills, "Trickle-Bed Reactors: Dynamic Tracer Tests, Reaction Studies, and Modeling of Reactor Performance," *Chemical Reaction Engineering—Boston*, J. Wei and C. Georgakis, eds., *Am. Chem. Soc. Symp. Ser.*, No. 196, 421 (1982).
- Fukushima, S., and K. Kusaka, "Liquid-Phase Volumetric and Mass Transfer Coefficient, and Boundary of Hydrodynamic Flow Region in Packed Column with Concurrent Downward Flow," *J. Chem. Eng. Japan*, **10**, 468 (1977).
- Goto, S., A. Lakota, and J. Levec, "Effectiveness Factors of n th Order Kinetics in Trickle-Bed Reactors," *Chem. Eng. Sci.*, **36**, 157 (1981).
- Harriott, P., private communication with P. L. Mills (Oct. 8, 1984).
- Herskowitz, M., "Wetting Efficiency in Trickle-Bed Reactors. The Overall Effectiveness Factor of Partially Wetted Catalyst Particles," *Chem. Eng. Sci.*, **36**, 1665 (1981).
- Herskowitz, M., R. G. Carbonell, and J. M. Smith, "Effectiveness Factors and Mass Transfer in Trickle-Bed Reactors," *AIChE J.*, **25**, 272 (1979).
- Herskowitz, M., S. Morita, and J. M. Smith, "Solubility of Hydrogen in α -methylstyrene," *J. Chem. Eng. Data*, **23**, 227 (1978).
- Levec, J., S. Pavko, and M. Dobovisek, "Effectiveness Factor for Partially Wetted Catalyst Particles," *Chem. Eng. Sci.*, **35**, 1815 (1980).
- Lu, P. Z., J. M. Smith, and M. Herskowitz, "Gas-Particle Mass Transfer in Trickle Beds," *AIChE J.*, **30**, 500 (1984).
- Martinez, O. M., G. F. Barreto, and N. O. Lemcoff, "Effectiveness Factor of a Catalyst Pellet in a Trickle-Bed Reactor. Limiting Reactant in the Gas Phase," *Chem. Eng. Sci.*, **36**, 901 (1981).
- Mata, A. R., and J. M. Smith, "Oxidation of Sulfur Dioxide in a Trickle-Bed Reactor," *Chem. Eng. J.*, **22**, 229 (1981).
- Mills, P. L., and M. P. Duduković, "Analysis of Catalyst Effectiveness in Trickle-Bed Reactors Processing Volatile or Nonvolatile Reactants," *Chem. Eng. Sci.*, **35**, 2267 (1980).
- , "A Comparison of Current Models for Isothermal Trickle-Bed Reactors. Application to a Model Reaction System," *Chemical and Catalytic Reactor Modeling*, M. P. Duduković and P. L. Mills, eds., *Am. Chem. Soc. Symp. Ser.*, No. 237, 37 (1984).
- Mills, P. L., E. G. Beaudry, and M. P. Duduković, "Comparison and Prediction of Reactor Performance for Packed Beds with Two-Phase Flow: Downflow, Upflow, and Countercurrent Flow," *Inst. Chem. Eng. Symp. Ser.*, No. 87, 527 (1984).
- Morita, S., and J. M. Smith, "Mass Transfer and Contacting Efficiency in a Trickle-Bed Reactor," *Ind. Eng. Chem. Fundam.*, **17**, 113 (1978).
- Morrison, T. J., and F. Billett, "The Salting-out of Non-Electrolytes. II: The Effect of Variation in Non-Electrolytes," *J. Chem. Soc.*, **57**, 3819 (1952).
- Ramachandran, P. A., and J. M. Smith, "Effectiveness Factors in Trickle-Bed Reactors," *AIChE J.*, **25**, 538 (1979).
- Reid, R. C., J. M. Prausnitz, and T. K. Sherwood, *The Properties of Gases and Liquids*, McGraw-Hill, New York (1977).
- Ring, Z. E., and R. W. Missen, "Trickle-Bed Reactors: Effect of Wetting Geometry on Overall Effectiveness Factor," 34th Can. Chem. Eng. Conf., Quebec (1984).
- Ruiz, P., M. Crine, A. Germain, and G. L'Homme, "Influence of the Reactional System on the Irrigation Rate in Trickle-Bed Reactors," *Chemical and Catalytic Reactor Modeling*, M. P. Duduković and P. L. Mills, eds., *Am. Chem. Soc. Symp. Ser.*, No. 237, 15 (1984).
- Sakornwimon, W., and N. D. Sylvester, "Effectiveness Factors for Partially Wetted Catalysts in Trickle-Bed Reactors," *Ind. Eng. Chem. Process Des. Dev.*, **21**, 16 (1982).
- Tan, C. S., and J. M. Smith, "Catalyst Particle Effectiveness with Unsymmetrical Boundary Conditions," *Chem. Eng. Sci.*, **35**, 1601 (1980).
- , "A Dynamic Method for Liquid-Particle Mass Transfer in Trickle Beds," *AIChE J.*, **28**, 190 (1982).
- Wilhelm, E., and R. Battino, "Thermodynamic Functions of the Solubilities of Gases in Liquids at 25°C," *Chem. Rev.*, **73**, (1973).

Manuscript received Nov. 3, 1986, and revision received Mar. 12, 1987.